JOURNAL OF AGRICULTURAL AND FOOD CHEMISTRY

pubs.acs.org/JAFC Article

New Insights into Decabromodiphenyl Ether-Induced Splenic Injury in Chickens: Involvement of ROS-Mediated Endoplasmic Reticulum Stress Pathway Triggering Autophagy and Apoptosis

Bendong Shi, Bowen Dong, Jianhua Shan, Zhuoqi Zhang, Qiaohan Liu, Yangyang Jiang, Cheng Fang, Jingzeng Cai, and Ziwei Zhang*

Cite This: *J. Agric. Food Chem.* 2024, 72, 3741−3754 Read Online

ACCESS | Metrics & More | Article Recommendations | Supporting Information

ABSTRACT: Decabromodiphenyl ether (BDE-209) is a widely used brominated flame retardant that can easily detach from materials and enter into feed and foodstuffs, posing a serious risk to human and animal health and food safety of animal origin. However, the immunotoxic effects of BDE-209 on the avian spleen and the exact mechanism of the toxicity remain unknown. Therefore, we established an experimental model of BDE-209-exposed chickens and a positive control model of cyclophosphamide-induced immunosuppression in vivo and treated MDCC-MSB-1 cells and chicken splenic primary lymphocytes with BDE-209 in vitro. The results showed that BDE-209 treatment caused morphological and structural abnormalities in the chicken spleens. Mechanistically, indicators related to oxidative stress, endoplasmic reticulum stress (ERS), autophagy, and apoptosis were significantly altered by BDE-209 exposure in both the spleen and lymphocytes, but the use of the *N*-acetylcysteine or the 4-phenylbutyric acid significantly reversed these changes. In addition, BDE-209 exposure decreased the spleen antimicrobial peptide and immunoglobulin gene expression. In conclusion, the present research revealed that BDE-209 exposure enhanced lymphocyte autophagy and apoptosis in chicken spleen via the ROS-mediated ERS pathway. This signaling cascade regulatory relationship not only opens up a new avenue for studying BDE-209 immunotoxicity but also provides important insights into preventing BDE-209 hazards to animal health.

KEYWORDS: *decabromodiphenyl ether, ERS, autophagy, apoptosis, chicken spleen, oxidative stress*

1. INTRODUCTION

Polybrominated diphenyl ethers (PBDEs) represent a vital cluster of brominated flame retardants extensively used in various products for their prominent flame retardant abilities and cost-effectiveness. As additives in products, PBDEs are prone to enter various environmental media through volatilization and exudation pathways due to their lack of chemical bond binding.[1] Decabromodiphenyl ether (BDE-209) is a congener of PBDEs, and is accountable for roughly 82% of its entire production, acting as the most contaminating monomer congener of PBDEs found in China.[2] BDE-209 has been found in environmental samples globally, and an estimated 50% of feed samples for livestock contain BDE-209 contamination.[3] PBDEs were detected at 81.8−695.5 pg g^{-1} in the eastern part of Antarctica, with BDE-209 being the highest detected congener.[4] Detection of BDE-209 is the most highly detected congener of PBDEs in sediments from selected coastal waters of Japan and Korea.[5,6] Ji et al. reported that the concentration of PBDEs in dust in parts of the Pearl River Delta in China reached a maximum of 40,236 ng/g, of which 95.1% was BDE-209.[7] Meanwhile, studies have reported serum concentrations of BDE-209 in occupational workers ranging from 67.4 to 109,000 ng/g lipid weight, suggesting that humans are also inadvertently ingesting higher levels of BDE-209.[8] According to reports, BDE-209 has a propensity to accumulate in several organisms through the food chain due to its low biodegradability and long half-life, causing irreversible toxic damage to various biological organs. After oral administration of BDE-209 in male broilers, BDE-209 could be widely distributed in tissues such as the liver, thymus, lungs, kidneys, spleen, and testes through intestinal absorption, leading to systemic multiple organ toxicology exposures.[9] Li et al. demonstrated that BDE-209 diminished both the quality and quantity of sperm through oxidative stress-induced DNA damage and apoptosis of testicular cells in mice.[10] Exposure to BDE-209 during pregnancy in mice can cause ERS and apoptosis in placental tissue.[11] Excessive reactive oxygen species (ROS) and endoplasmic reticulum stress (ERS) elicited by BDE-209 could result in activating excessive autophagy, eventually leading to programmed cell death in HUVEC cells.[12] Furthermore, Che et al. demonstrated that BDE-209 initiated apoptosis by inducing ERS, thereby disrupting calcium homeostasis in mouse liver.[13] Nevertheless, mechanistic studies on the effects of BDE-209 on the avian spleen and immune function are still lacking.

Received: December 4, 2023
Revised: January 27, 2024
Accepted: January 30, 2024
Published: February 10, 2024

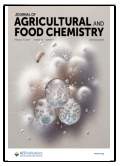

The occurrence of oxidative stress shows that the ability of oxidation and antioxidation is not balanced, and the damage to immune function is closely related to its occurrence. Polystyrene microplastics induce thymus injury in chickens through oxidative stress, triggering autophagy and apoptosis.[14] In addition, exposure to ammonia in broilers induces oxidative stress and apoptosis, thereby influencing the immune function of the bursa of fabricius.[15] In addition to oxidative stress, ERS has also been proven to be involved in the regulation of immune function.[16] The endoplasmic reticulum (ER) is a highly dynamic organelle within cells that plays an important role in protein folding, modification, and calcium homeostasis maintenance. Disruption from numerous adverse stimuli both inside and outside of the cell results in an imbalance of ER folding capacity, leading to protein misfolding and the accumulation of unfolded proteins that induce ERS. During ERS, three types of ER transmembrane proteins (ATF6, IRE1, and PERK) regulate the associated signal pathways to commence the adaptive unfolded protein response (UPR). The UPR could relieve ERS and maintain ER function, but severe or long-term ERS induces cell "suicide", usually in the form of apoptosis. Chronic exposure to copper in pigs has been reported to cause the induction of apoptosis in splenocytes, resulting from ERS.[17] Co-exposure of molybdenum and cadmium leads to spleen injury in ducks by activating ERS-mediated apoptosis.[18] Perinatal low-dose BDE-47 exposure can trigger ERS and induce thyroid cell apoptosis in rats.[19] Furthermore, ERS is closely associated with the activation of autophagy.[20] Autophagy is an evolutionarily conservative catabolism process, which can control cell fate through different crosstalk signals.[21] Scientific researchers have proven that adverse factors inducing excessive autophagy could exacerbate tissue damage.[22] PERK and GRP78 are important regulators of autophagy induced by ERS.[23] IRE1 protein is also able to trigger autophagy by regulating the mTOR signaling pathway.[24] Li et al. have shown that exposure to particulate matter initiates autophagy via induction of ERS, resulting in damage to the bronchial epithelium.[25] Liu et al. demonstrated that BDE-47 inhibits the early development of porcine embryos through autophagy mediated by ERS.[26] However, whether the effect of BDE-209 treatment on splenic immune function is related to ERS-regulated autophagy and apoptosis has not been elucidated.

As an immune organ, the spleen can regulate various immune responses and plays a crucial role in maintaining the body's immune function. Immune organ stress, apoptosis, and autophagy are considered to form the foundation for the development of numerous immune system diseases.[27,28] Several studies have shown that exposure to BDE-209 and its congeners can cause damage to a variety of biological immune organs by inducing oxidative damage and disturbing immune homeostasis.[29,30] However, whether BDE-209 exposure-induced splenic injury in broilers is associated with ROS-mediated ERS pathways driving autophagy and apoptosis is not known. In this study, we established an experimental model of broiler chickens exposed to different concentrations of BDE-209 and a positive control model of chicken immunosuppression in vivo. We observed the occurrence of ERS, apoptosis, and autophagy in the spleen by hematoxylin-eosin staining (H&E), transmission electron microscopy (TEM), terminal deoxynucleotidyl transferase dUTP nick labeling (TUNEL) staining, and immunofluorescence. The mRNA and protein expression levels within associated pathways were determined through qRT-PCR and Western blot analysis. Concurrently, chicken lymphoma cells and primary spleen lymphocytes from broilers in vitro were cultured to investigate the correlation between ERS, autophagy, and apoptosis when exposed to BDE-209. In conclusion, the purpose of our study was to elucidate the mechanisms underlying BDE-209's impact on splenic immunotoxicity in broilers. This research provides essential information for the environmental risk assessment of BDE-209 and fills in knowledge gaps concerning BDE-209 exposure and its effects on poultry splenotoxicity.

2. MATERIALS AND METHODS

2.1. Animals and Treatments. 75 Hy-Line white-feathered chicks (1 day old) were purchased from Xianfeng hatchery (Harbin, China). BDE-209 powder (>98% purity) was purchased from Macklin Biotechnology Co., Ltd. Cyclophosphamide (CTX, purity >97%, CAS number: 6055-19-2) was purchased from Shanghai Yuanye Biotechnology Co., Ltd. The intragastric working solution was prepared by dissolving BDE-209 powder in corn oil (Macklin Biotechnology Co., Ltd., shanghai, China). All animal experiments are conducted in strict compliance with the applicable regulations of Northeast Agricultural University's Experimental Animal Ethics Committee (NEAUEC202376). Before the experiment, the chicks were fed adaptively for 7 days under standard laboratory conditions. One week later, the chicks were randomly divided into five groups: CON group, L-BDE209 group, M-BDE209 group, H-BDE209 group, and CTX group. L-BDE209, M-BDE209, and H-BDE209 groups were orally gavaged with 40 mg/kg/d, 400 mg/kg/d, and 4 g/kg/d of BDE-209, respectively, while the CON group was orally gavaged with the same amount of corn oil. Chicks in the CTX group were subjected to immunosuppression through intramuscular injection of cyclophosphamide at a dose of 80 mg/kg/d on days 11 to 13. After 42 days of exposure, the chickens in the five groups were euthanized, and their spleen tissues were promptly harvested. A portion of the spleen was preserved at −80 °C for future study, while the remainder was fixed with 4% paraformaldehyde or 2.5% glutaraldehyde for follow-up tissue section and transmission electron microscope observation. The BDE-209 concentration and CTX injection dose used in our experiment were determined concerning previous studies.[31−33] It has been reported that the toxicological effects of subchronic ingestion of environmental pollutants on organisms may not be as significant as expected, and higher environmental exposure concentrations are more suitable for toxicological research and judgment.[34] Considering the rapid metabolism of poultry, this experiment used a 10-fold concentration gradient to study the toxicological effects of poultry.[35]

2.2. Hematoxylin and Eosin (H&E) Staining. H&E staining was utilized to evaluate morphological alterations in the spleens of chickens following exposure to varying doses of BDE-209, and the methodology was referenced from prior studies.[36] Briefly, each group of chicken spleen tissues needed to go through a series of steps, such as fixation, embedding, sectioning, dehydration, dewaxing, staining, and sealing. Finally, a light microscope (Nikon 80i, Nikon Corporation, Japan) was used to observe the pathological changes.

2.3. TEM Observation. Fresh splenic tissues were divided into squares of less than 1 mm^3 and fixed in a 2.5% glutaraldehyde solution for at least 48 h. Then, the samples were processed and stained according to the study by Jiang et al.[37] Finally, the ultramicrostructure of the spleen was observed through TEM (GEM-1200ES, Japan).

2.4. Cell Line and Primary Splenic Lymphocyte Culture and Treatment. In vitro testing was conducted using the chicken lymphoma cell line MDCC-MSB-1 cells and chicken primary splenic lymphocytes. Spleens from 4-week-old broilers were used to extract primary lymphocytes. The detailed extraction steps and experimental conditions refer to the introduction of previous studies.[38] MDCC-MSB-1 cells and primary lymphocytes were inoculated into RPMI-1640 medium (Gibco, Shanghai, China) containing 10% fetal bovine serum (VivaCell, Shanghai, China) and 1% penicillin-streptomycin

https://doi.org/10.1021/acs.jafc.3c09104
J. Agric. Food Chem. 2024, 72, 3741−3754

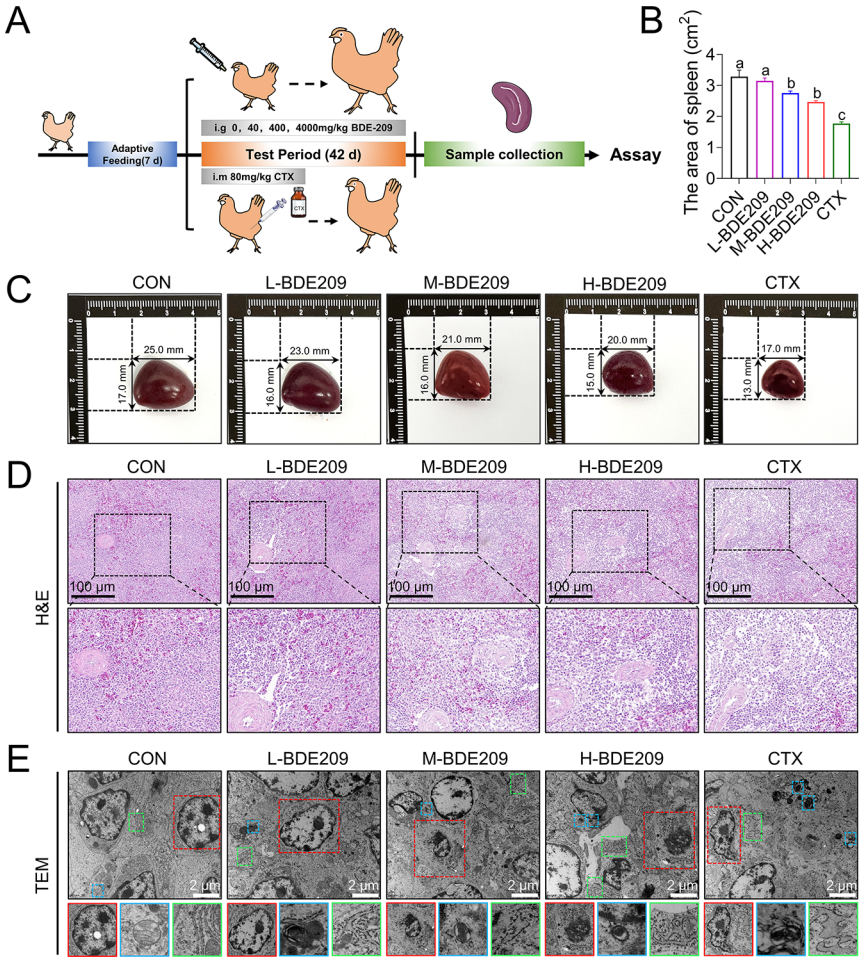

Figure 1. BDE-209 exposure-induced splenic injury in chickens. (A) Experimental period chart. (B) Quantification of spleen area in different treatment groups. (C) Picture of chicken spleen morphology. (D) H&E staining sections of the chicken spleen. Scale bar: 100 μm. (E) Ultrastructure of chicken spleen lymphocytes. Scale bar: 2 μm. The red frames indicate the cell nucleus. Blue frames indicate autophagic vacuoles. The green frames indicate ER expansion (magnification 15,000×). The data are expressed as means ± SD. Samples indicated a statistically significant difference when represented by distinct superscript letters ($P < 0.05$).

(Procell Life Science & Technology Co., Ltd., Wuhan, China) and cultured in a cell incubator containing 5% CO_2 at 37 °C. The viability of MDCC-MSB-1 cells was assessed using the commercial CCK-8 kit (Saint-Bio, Shanghai) after exposing them to varying concentrations of BDE-209. In the study of cell injury induced by BDE-209, MDCC-MSB-1 cells were treated with BDE-209 at 0, 1/4, 1/2, and 3/4 times the IC_{50} concentration, respectively. The primary lymphocytes of the spleen were treated with the same BDE-209 concentration as MDCC-MSB-1 cells to verify the type of damage. Briefly, both the MDCC-MSB-1 cell and primary lymphocyte experiments were divided into four groups: CON group, L-BDE209 (80 μM) group, M-BDE209 (160 μM) group, and H-BDE209 (240 μM) group. N-Acetylcysteine (NAC, MedChemExpress, America) and 4-phenylbutyricacid (4-PBA, MedChemExpress, America) are scavengers of ROS and specific inhibitors of ERS, respectively. In salvage experiments, the altered ROS and ERS levels play an important role in BDE-209-induced spleen injury. Before the cells were treated with BDE-209, they were pretreated with NAC (0.5 mM for 1 h) or 4-PBA (1 mM for 1 h). Then, cells were cotreated with BDE-209 with NAC (0.5 mM) or 4-PBA (1 mM) for 24 h.

2.5. Oxidative Stress Analysis. The spleen tissue was ground into homogenates, centrifuged, and the supernatant was aspirated for kit detection. Similarly, MDCC-MSB-1 cells were sonicated and centrifuged to obtain the supernatant. The activity or content of MDA (A003-1-2), T-AOC (A015-1-2), T-SOD (A001-3-2), CAT (A007-1-1), GSH (A005-1-2), and GSH-Px (A005-1-2) in the spleen or MDCC-MSB-1 cells was measured using a commercially available assay kit (Nanjing Jiancheng Bioengineering Institute, China). A commercial DCFH-DA fluorescent probe kit (Nanjing Jiancheng Bioengineering Institute, China) was used to detect intracellular ROS accumulation.[39] Serum-free medium containing the DCFH-DA probe was added to both MDCC-MSB-1 cells and primary spleen lymphocytes that had undergone distinct treatments and incubated in the dark for 30 min under appropriate conditions. Finally, a fluorescent inverted microscope (Olympus IX53, Japan) was used to capture images.

2.6. Apoptosis Analysis. *2.6.1. TdT-Mediated dUTP Nick-End Labeling (TUNEL) Staining.* TUNEL staining was used to examine the effects of BDE-209 exposure or CTX treatment on the rate of apoptosis in the broiler spleen cells. Briefly, 4% paraformaldehyde-fixed spleen tissue was embedded and sectioned. Tissue sections were then stained in strict accordance with the instructions of the commercial kit (Roche, Switzerland). At the same time, 100 μg/L DAPI (Beyotime Biotechnology, China) was used to stain the nuclei of all of the cells in the spleen. Finally, fluorescence images were collected via a fluorescent inverted microscope (Olympus, IX53, Japan).

2.6.2. Acridine Orange/Ethidium Bromide (AO/EB) Dual Staining. The operational procedure is executed in strict accordance with the guidelines provided by the commercial AO/EB staining kit (Beyotime Biotechnology, China). Briefly, after cells were treated differently, AO/EB working solution (10 μL/mL) was added for staining for 5 min.[40] Finally, fluorescence images were collected by a fluorescent inverted microscope (Olympus, IX53, Japan).

https://doi.org/10.1021/acs.jafc.3c09104
J. Agric. Food Chem. 2024, 72, 3741−3754

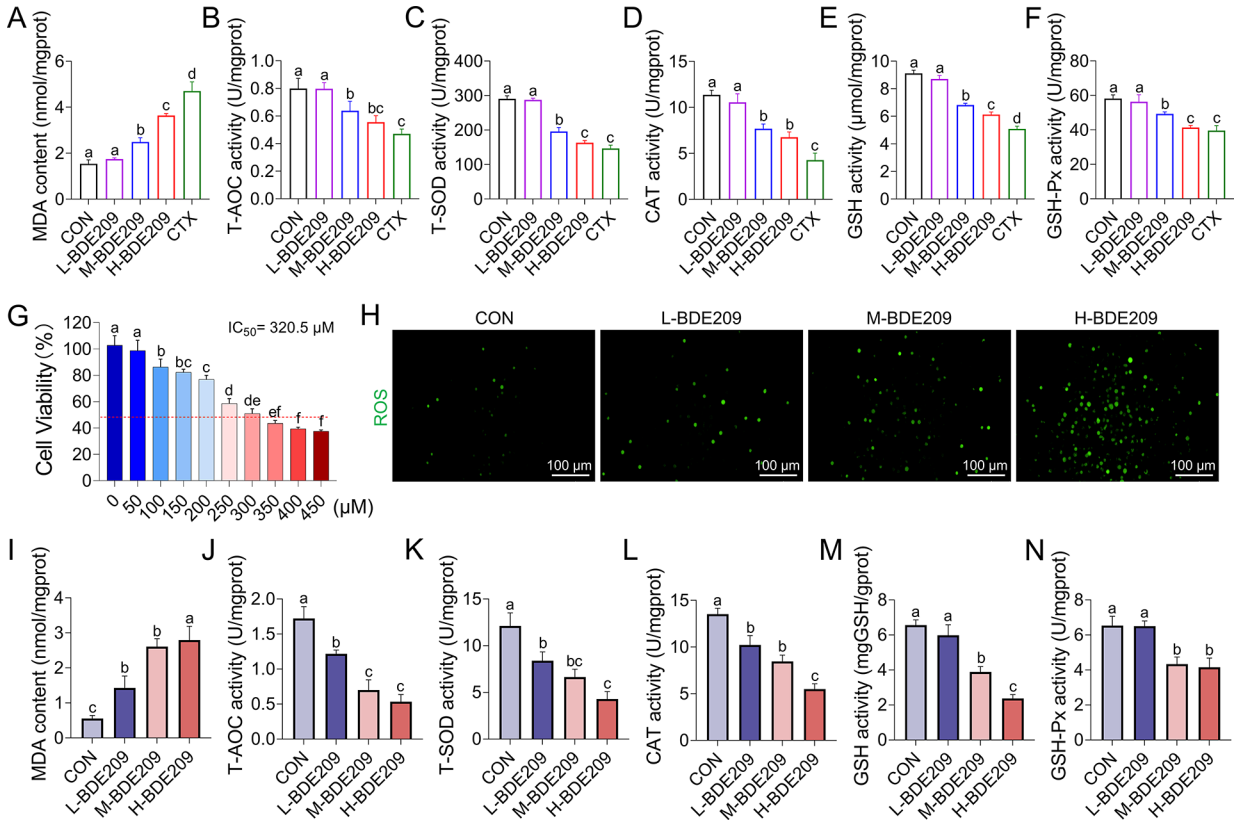

Figure 2. BDE-209 exposure-induced oxidative stress in spleen tissues and MDCC-MSB-1 cells. (A) The content of MDA in the spleen. (B−F) The activity of T-AOC, T-SOD, CAT, GSH, and GSH-Px in the spleen. (G) The effects of different concentrations of BDE-209 on the viability of MDCC-MSB-1 cells. (H) DCFH-DA staining was used to detect ROS accumulation. Scale bar: 100 μm. (I) The content of MDA in MDCC-MSB-1 cell. (J−N) The activity of T-AOC, T-SOD, CAT, GSH, and GSH-Px in the MDCC-MSB-1 cell. The data are expressed as means ± SD. Samples indicated a statistically significant difference when represented by distinct superscript letters ($P < 0.05$).

2.6.3. Hoechst 33342 Staining. MDCC-MSB-1 cells and primary splenic lymphocytes were seeded in 6-well plates and treated with different stimulations. Then Hoechst 33342 staining solution (Beyotime Biotechnology, China) was added to the cells of different treatment groups, and incubated for 30 min under the condition of avoiding light at 37 °C.[41] Finally, images were collected by a fluorescent inverted microscope (Olympus, IX53, Japan).

2.7. Immunofluorescence (IF) Staining. In this experiment, the steps for immunofluorescence double staining of spleen tissue sections were based on previous studies.[42] Briefly, spleen sections were incubated with primary antibodies for LC3, Beclin-1, GRP78, and PERK overnight at 4 °C. After washing with TBST, the sections were incubated with the corresponding fluorescent secondary antibody for 1 h. DAPI was used to counter-stain cell nuclei before mounting. In the cell immunofluorescence experiment, the cell culture plate was first coated with polylysine, and then the MDCC-MSB-1 cell suspension was seeded into a 12-well plate. Cells were fixed with 4% paraformaldehyde after different treatments and then blocked with a blocking solution for 2 h at 25 °C. The cells were incubated overnight at 4 °C with primary antibodies against LC3, Beclin-1, GRP78, and PERK, respectively, and then incubated with fluorescent secondary antibodies against AbBox Fluor 488 (1:1000, Biodragon, China) or Dylight 594 (1:1000, Biodragon, China) for 60 min, respectively. Cell nuclei were stained with DAPI for 5 min, washed with TBST, and an antifluorescence quenching mounting solution was added dropwise. Finally, fluorescence images were collected through a fluorescent inverted microscope (Olympus, IX53, Japan), and ImageJ software (National Institutes of Health, Bethesda, USA) was used to quantitatively analyze the fluorescence intensity of each group.

2.8. RNA Extraction and Real-Time Quantitative PCR (qRT-PCR). Total RNA was extracted from the chicken spleen, MDCC-MSB-1 cells, and primary splenic lymphocytes using the TRizol (BioFlux, USA) method. A commercial reverse transcription kit (Bioer Technology, China) was used to reverse transcribe the extracted RNA into cDNA. Then, the Fast SYBR Green Master Mix kit (Bioer Technology, China) was used to detect the mRNA expression level. β-actin was used as the internal reference gene, and the $2^{-\Delta\Delta Ct}$ method was used to process the data statistically. The primer sequences used in this experiment were designed and synthesized by Sangon Biotech (Table S1).

2.9. Protein Extraction and Western Blotting. For Western blot analysis, the total proteins of spleen tissue, MDCC-MSB-1 cells, and primary spleen lymphocytes were extracted with RIPA lysate (including the PMSF protease inhibitor). Protein samples were separated by an SDS-PAGE gel and transferred to the NC membrane. The NC membrane was placed in a blocking solution containing 5% skim milk, blocked at room temperature for 2 h, and then incubated with the corresponding primary antibody at 4 °C overnight (Table S2). TBST was used to wash the remaining primary antibodies on the membrane surface and then the NC membrane was incubated with HRP-labeled secondary antibodies (goat antirabbit or goat antimouse, Abbkine Biotechnology, Wuhan, China) at 37 °C for 60 min. Images were collected using an Image QuantLAS4000 digital imaging system, and ImageJ software (National Institutes of Health, Bethesda, USA) was used to analyze the gray value of the corresponding protein bands.

2.10. Statistical Analysis. SPSS 18.0 software (SPASS, IL, USA) was used to analyze the experimental data and express them as means ± SD. All data were analyzed using a one-way ANOVA, followed by Tukey's post hoc test and Student's *t*-test. GraphPad Prism 9 software (GraphPad Software Inc., San Diego, CA) was used for graphing. The same superscript letter indicates no significant difference ($P > 0.05$),

https://doi.org/10.1021/acs.jafc.3c09104
J. Agric. Food Chem. 2024, 72, 3741−3754

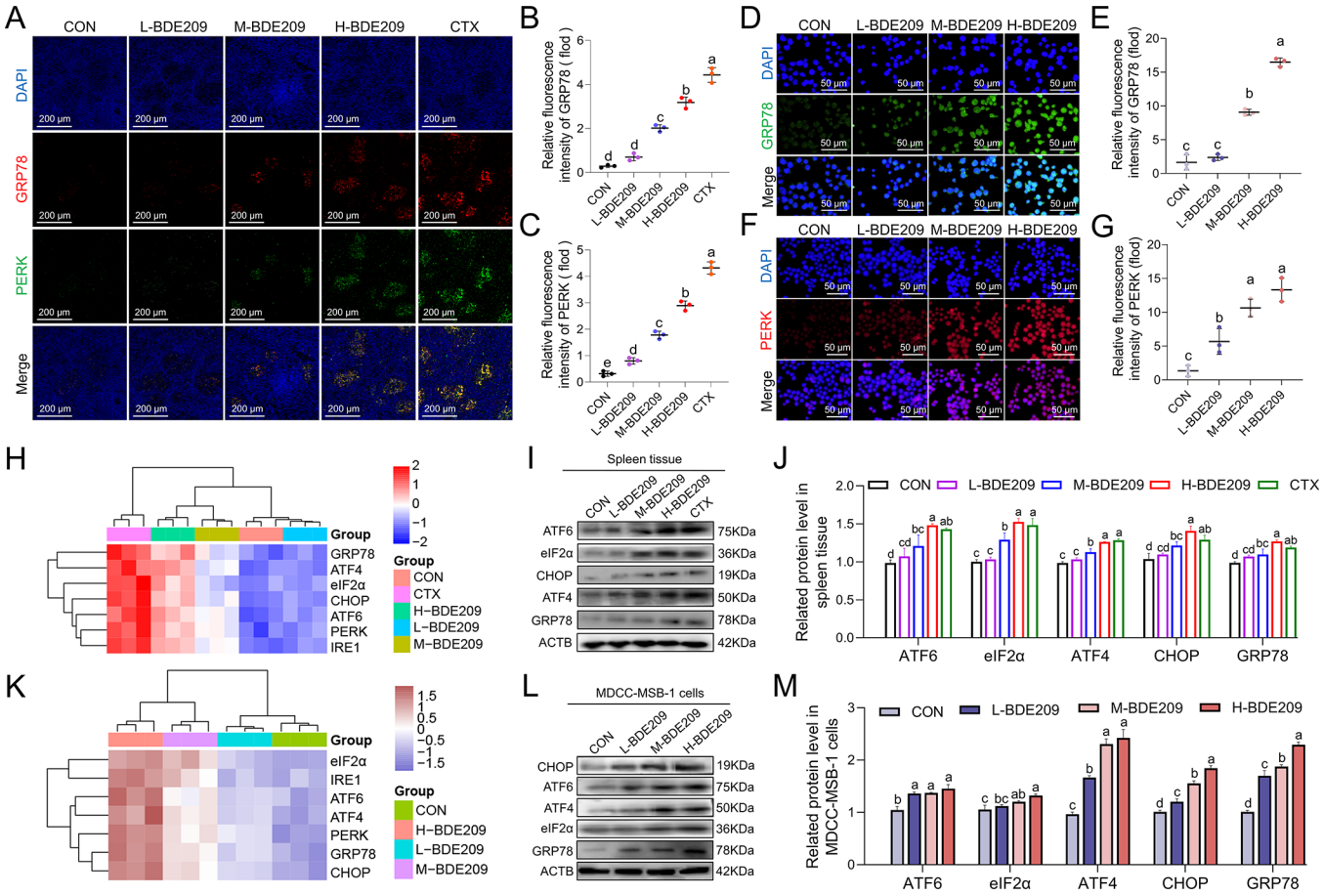

Figure 3. BDE-209 exposure-induced ERS in spleen and MDCC-MSB-1 cells. (A) Immunofluorescence of GRP78 (red) and PERK (green) proteins in spleen tissue. Scale bars: 200 μm. (B) Relative fluorescence intensity of GRP78 in spleen. (C) Relative fluorescence intensity of PERK in spleen. (D) Representative immunofluorescence images of the GRP78 protein in MDCC-MSB-1 cells. Scale bars: 50 μm. (E) Relative fluorescence intensity of GRP78 in MDCC-MSB-1 cells. (F) Representative immunofluorescence images of the PERK protein in MDCC-MSB-1 cells. Scale bars: 50 μm. (G) Relative fluorescence intensity of PERK in MDCC-MSB-1 cells. (H) Heat map of mRNA clustering of ERS-related genes in the spleen. (I,J) Western blot analysis of the levels of ERS-related proteins (ATF6, eIF2α, CHOP, ATF4, and GRP78) in chicken spleen. (K) Heat map of mRNA clustering of ERS-related genes in MDCC-MSB-1 cells. (L,M) Western blot analysis of the levels of ERS-related proteins (ATF6, eIF2α, CHOP, ATF4, and GRP78) in MDCC-MSB-1 cells. The data are expressed as means ± SD. Samples indicated a statistically significant difference when represented by distinct superscript letters ($P < 0.05$).

and a different superscript letter indicates a statistically significant difference between groups ($P < 0.05$).

3. RESULTS

3.1. BDE-209 Exposure Induces Splenic Injury and Reduces Immune Function in Chickens. The specific experimental period and technical process are listed in Figure 1A. The spleen area of the M-BDE209, H-BDE209, and CTX groups was significantly lower than that of the CON group (Figure 1B,C). The pathological damage of spleen tissue induced by BDE-209 and CTX was evaluated by H&E staining (Figure 1D). Pathological observation revealed that the spleen shape of broiler chickens in the control group was within normal, featuring distinct boundaries between white and red pulp, closely aligned lymphocytes, and no obvious abnormalities in the splenic corpuscles and arteries. The damage types in both the BDE-209 and CTX groups shared similarities. They all exhibited a degree of white pulp and red pulp mixing, leading to unclear boundaries, reduced lymphocyte counts with loose organization, and loosely arranged tissue around the splenic artery. TEM results demonstrate that the nuclear chromatin of the cells in the CON group was uniform with complete cell membranes and nuclear membranes, and the ER had normal morphology and clear structure. The group with CTX exhibited nuclear pyknosis, chromatin condensation, expansion of the ER lumen, an elevated count of autophagosomes, and the existence of apoptotic bodies. The type of injury in the BDE-209 group resembled that of the CTX group, exhibiting varying degrees of expansion in the ER lumen, increased instances of autophagosomes, and cell apoptosis (Figure 1E). CTX treatment significantly downregulated the levels of antimicrobial peptides and immunoglobulin mRNA in the spleen. The middle and high doses of BDE-209 exposure were similar to those of CTX treatment, and the mRNA expression of the above indexes in the spleen was downregulated in varying degrees (Figure S1).

3.2. BDE-209 Exposure-Induced Oxidative Stress in Spleen and MDCC-MSB-1 Cells. We first examined the production of antioxidants and superoxide in the spleen tissue during BDE-209 treatment. As shown in Figure 2A−F, the MDA content of the BDE-209 exposure group and CTX group increased significantly, while BDE-209 and CTX treatment could significantly inhibit the activity of major antioxidant enzymes (T-AOC, T-SOD, CAT, GSH, and GSH-Px).

https://doi.org/10.1021/acs.jafc.3c09104
J. Agric. Food Chem. 2024, 72, 3741−3754

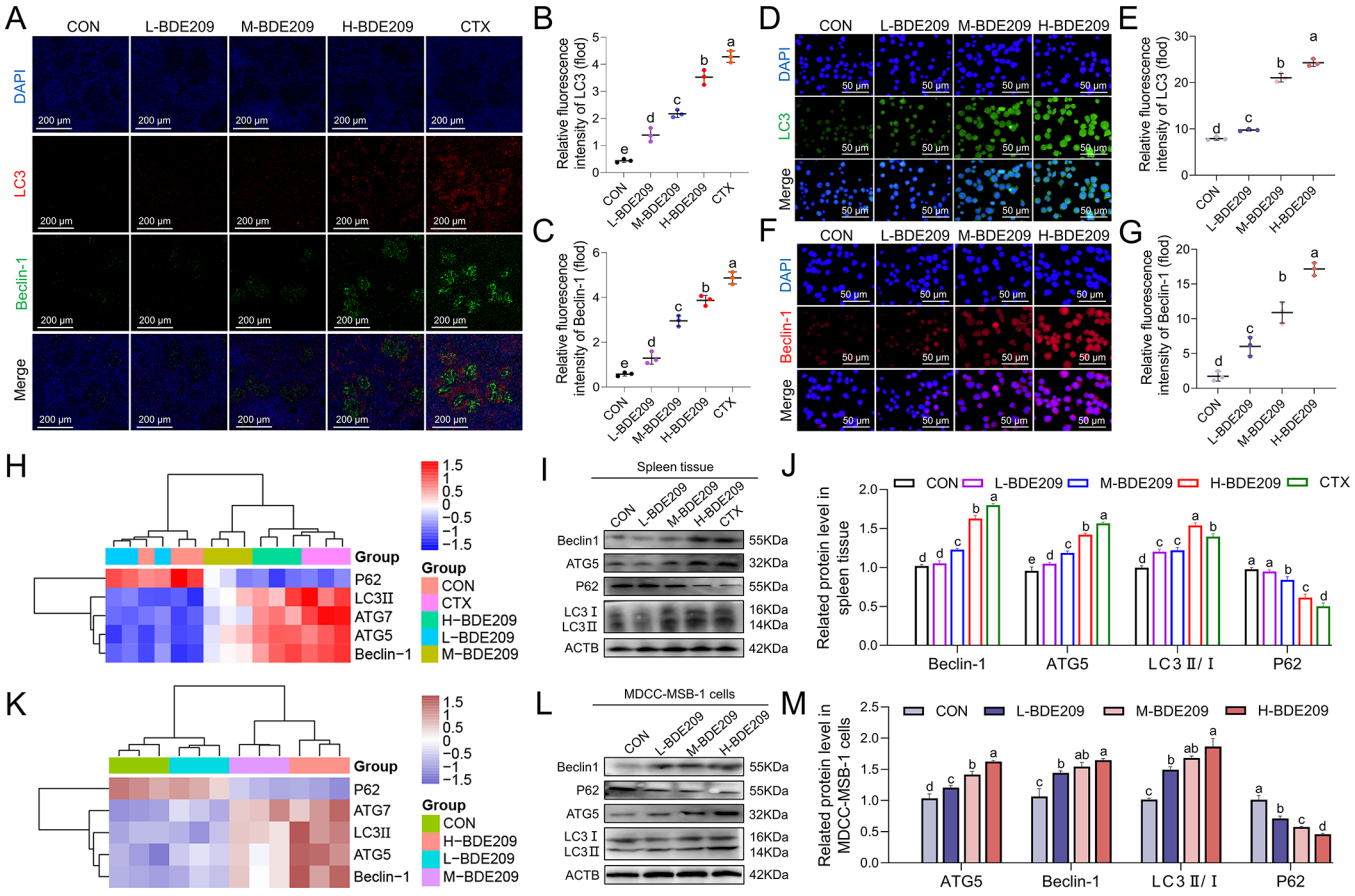

Figure 4. BDE-209 exposure triggers autophagy in spleen and MDCC-MSB-1 cells. (A) Immunofluorescence of LC3 (red) and Beclin-1 (green) proteins in spleen tissue. Scale bar: 200 μm. (B) Relative fluorescence intensity of LC3 in the spleen. (C) Relative fluorescence intensity of Beclin-1 in the spleen. (D) Representative immunofluorescence images of the LC3 protein in MDCC-MSB-1 cells. Scale bar: 50 μm. (E) Relative fluorescence intensity of LC3 in MDCC-MSB-1 cells. (F) Representative immunofluorescence images of the Beclin-1 protein in MDCC-MSB-1 cells. Scale bar: 50 μm. (G) Relative fluorescence intensity of Beclin-1 in MDCC-MSB-1 cells. (H) Heat map of mRNA clustering of autophagy-related genes in spleen. (I,J) Western blot analysis of the expression of autophagy-related proteins (Beclin-1, P62, ATG5, and LC3) in chicken spleen. (K) Heat map of mRNA clustering of autophagy-related genes in MDCC-MSB-1 cells. (L,M) Western blot analysis of the expression of autophagy-related proteins (Beclin-1, P62, ATG5, and LC3) in MDCC-MSB-1 cells. The data are expressed as means ± SD. Samples indicated a statistically significant difference when represented by distinct superscript letters ($P < 0.05$).

Interestingly, with the increase of the BDE-209 concentration, the changes of the above indicators were further aggravated. To further evaluate the effect of BDE-209 on lymphocytes in vitro, we treated cells with different concentrations of BDE-209. The survival rate of MDCC-MSB-1 cells decreased in a dose-dependent manner as the concentration of BDE-209 exposure increased. The IC_{50} of MDCC-MSB-1 cells after exposure to a medium containing BDE-209 for 24 h was 320.5 μM (Figure 2G). In vitro experiments show that the BDE-209 treatment can increase ROS production. In particular, the increase of ROS fluorescence intensity is overall dependent on the increase of BDE-209 exposure dose (Figure 2H). Similar to the in vivo findings, the content of MDA significantly increased in the BDE-209 exposure group, whereas the activity levels of antioxidant enzymes (T-AOC, T-SOD, CAT, GSH, and GSH-Px) markedly decreased (Figure 2I−N).

3.3. BDE-209 Exposure-Induced ERS in Spleen and MDCC-MSB-1 Cells. Based on the clues suggested by the results of TEM, both BDE-209 and CTX treatment could cause spleen ER swelling. Therefore, we measured the markers related to ERS in the spleen and MDCC-MSB-1 cells. As shown in Figure 3A−C, the spleen immunofluorescence double staining results showed that the fluorescence intensity of the GRP78 (red) and PERK (green) proteins in the spleen increased significantly after CTX treatment. Similarly, with the increase of BDE-209 exposure concentration, the fluorescence intensity of GRP78 (green) and PERK (red) proteins in spleen tissue was significantly higher than in the CON group. The immunofluorescence assay conducted on MDCC-MSB-1 cells demonstrated that exposure to BDE-209 led to a notable increase in the fluorescence intensity of GRP78 (green) and PERK (red) proteins in a dose-dependent way (Figure 3D−G). qRT-PCR results showed that exposure to BDE-209 or CTX treatment significantly increased the mRNA levels of ERS-related genes (GRP78, CHOP, ATF6, ATF4, PERK, IRE1, and eIF2α) in spleen or MDCC-MSB-1 cells (Figure 3H,K). Western blotting results showed that the levels of ERS-related proteins were significantly higher in the CTX group than in the CON group. Similarly, BDE-209 treatment also increased the protein expression levels of GRP78, ATF6, ATF4, CHOP, and eIF2α in spleen and MDCC-MSB-1 cells in a dose-dependent manner (Figure 3I,J,L,M).

3.4. BDE-209 Exposure-Induced Autophagy in Spleen and MDCC-MSB-1 Cells. To investigate the impact of BDE-209 or CTX treatment on the autophagy of spleen or MDCC-MSB-1 cells, we initially examined the markers of spleen

https://doi.org/10.1021/acs.jafc.3c09104
J. Agric. Food Chem. 2024, 72, 3741−3754

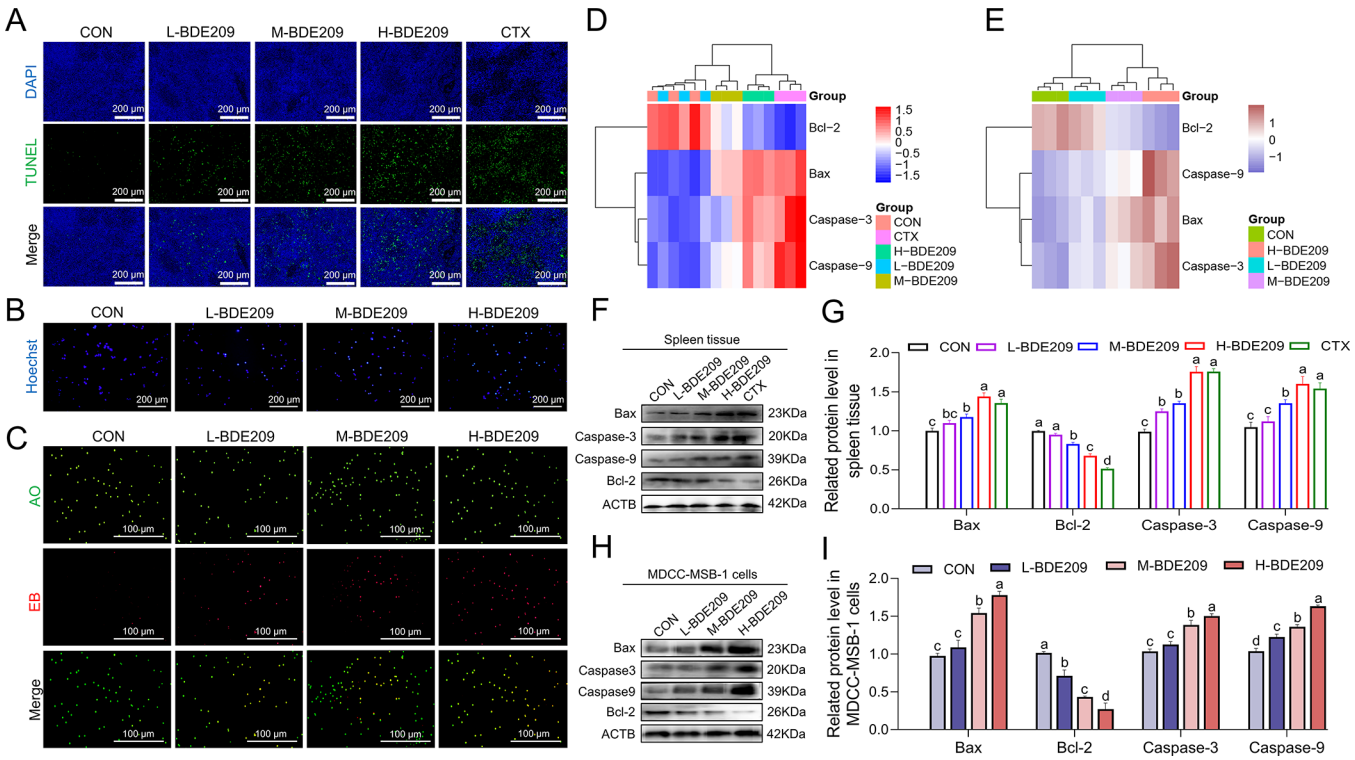

Figure 5. BDE-209 exposure-induced apoptosis in the spleen and MDCC-MSB-1 cells. (A) TUNEL staining was used to detect the apoptosis rate of spleen cells in each group. Scale bar: 200 μm. (B) Hoechst 33342 staining to detect apoptosis in MDCC-MSB-1 cells. (C) AO/EB staining to detect apoptosis in MDCC-MSB-1 cells. (D) Heat map of mRNA clustering of apoptosis-related genes in spleen. (E) Heat map of mRNA clustering of apoptosis-related genes in MDCC-MSB-1 cells. (F,G) Western blot analysis of the levels of apoptosis-related proteins (Bax, Caspase-3, Caspase-9, and Bcl-2) in chicken spleen. (H,I) Western blot analysis of the levels of apoptosis-related proteins (Bax, Caspase-3, Caspase-9, and Bcl-2) in MDCC-MSB-1 cells. The data are expressed as means ± SD. Samples indicated a statistically significant difference when represented by distinct superscript letters ($P < 0.05$).

autophagy (LC3 and Beclin-1) through immunofluorescence double staining. As illustrated in Figure 4A−C, the ratio of LC3-positive cells (red) and Beclin-1-positive cells (green) in the spleen of the CTX group was notably higher compared with the CON group. Interestingly, the ratio of LC3-positive cells (red) and Beclin-1-positive cells (green) in spleen tissue increased significantly with the BDE-209 treatment concentration compared with the CON group. The immunofluorescence results of MDCC-MSB-1 cells in vitro showed that BDE-209 exposure significantly increased the fluorescence intensity of LC3 (red) and Beclin-1 (green) proteins in a dose-dependent manner (Figure 4D−G). The results of the mRNA cluster heat map showed that BDE-209 exposure or CTX treatment could significantly upregulate the mRNA level of autophagy-related genes (Beclin-1, ATG5, and LC3) in spleen or MDCC-MSB-1 cells, while downregulate the mRNA level of P62 (Figure 4H,K). Western blotting results demonstrated that the levels of Beclin-1, ATG5, and LC3 proteins were significantly upregulated in the CTX group compared with the CON group. In contrast, the level of P62 protein was downregulated. Similarly, BDE-209 exposure also dose-dependently increased the levels of Beclin-1, ATG5, and LC3 in the spleen (Figure 4I,J) and MDCC-MSB-1 cells (Figure 4L,M), in contrast to the significant downregulation of p62 protein levels.

3.5. BDE-209 Exposure-Induced Apoptosis in Spleen and MDCC-MSB-1 Cells. The level of apoptosis could not be completely revealed by observing the ultrastructure of the spleen. Therefore, we first used TUNEL staining to evaluate the effect of BDE-209 or CTX treatment on spleen apoptosis in chickens. Compared with the CON group, CTX treatment could significantly increase the ratio of TUNEL-positive cells (green). Similarly, the ratio of TUNEL-positive cells (green) in the spleen increased with a BDE-209 exposure dose (Figure 5A). The results of Hoechst 33342 staining showed that the number of nuclear brightly stained cells increased with the increase in BDE-209 exposure concentration compared with the CON group (Figure 5B). Next, AO/EB staining was used to observe the effect of BDE-209 on MDCC-MSB-1 cells. As shown in the fluorescence image of Figure 5C, the normal cells are bright green, and the apoptotic cells are orange. BDE-209 treatment could increase the ratio of apoptotic MDCC-MSB-1 cells in a dose-dependent manner. The results of the mRNA clustering heat map of different treatment groups showed that compared with the CON group, the mRNA levels of proapoptotic genes Bax, Caspase-3, and Caspase-9 were significantly upregulated by BDE-209 or CTX, while the mRNA levels of antiapoptotic gene Bcl-2 were inhibited by BDE-209 or CTX (Figure 5D,E). Western blotting showed the same trend at the protein expression level, with either BDE-209 exposure or CTX treatment downregulating the levels of Bcl-2 protein and instead upregulating the levels of Bax, Caspase-3, and Caspase-9 in chicken spleen (Figure 5F,G) or MDCC-MSB-1 cells (Figure 5H,I).

3.6. NAC-Alleviated ERS, Autophagy, and Apoptosis Induced by BDE-209 Exposure in MDCC-MSB-1 Cells. To determine the role of ROS in BDE-209-induced MDCC-MSB-1 cell damage, we added the ROS scavenger NAC to stimulate

https://doi.org/10.1021/acs.jafc.3c09104
J. Agric. Food Chem. 2024, 72, 3741−3754

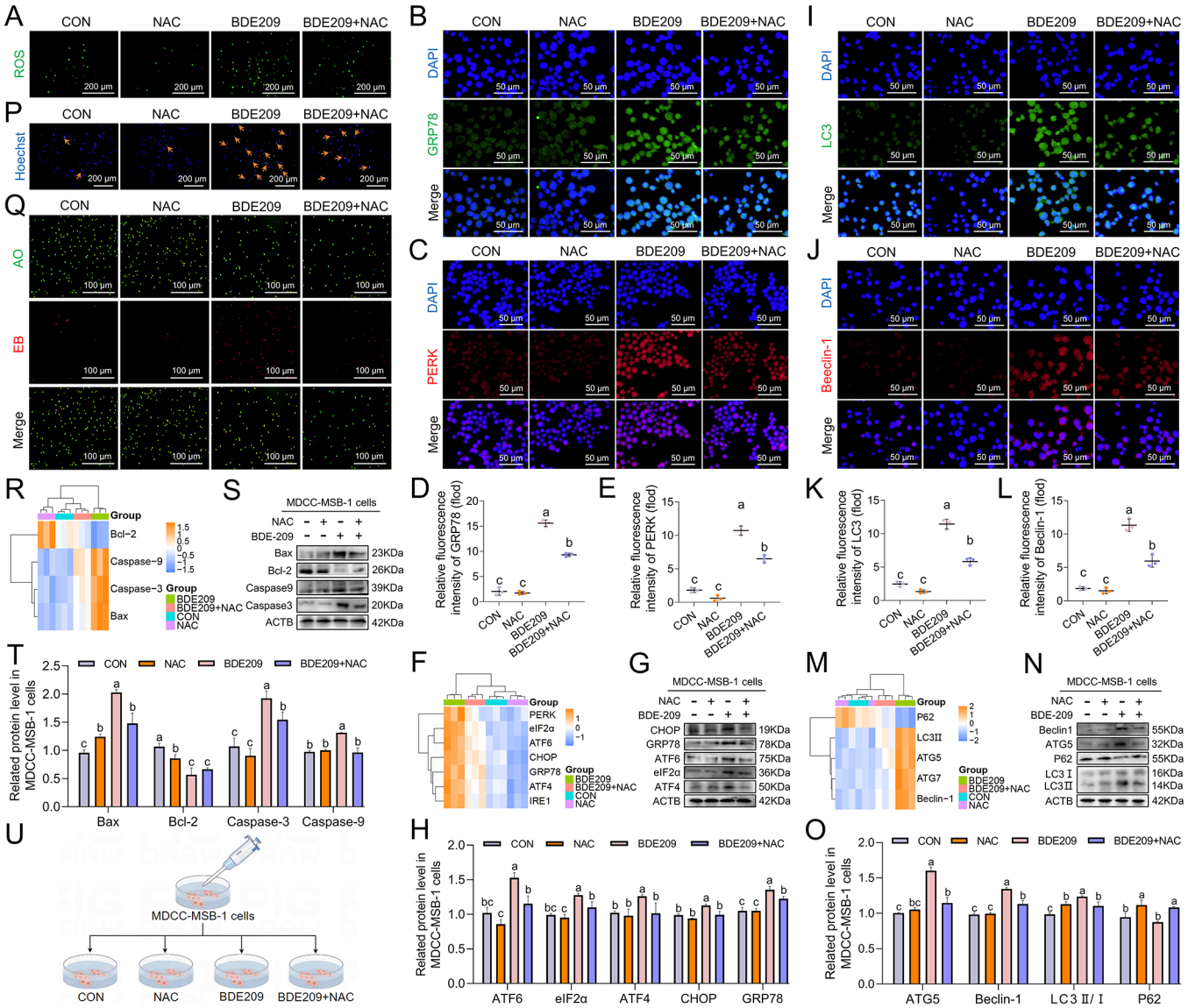

Figure 6. NAC inhibited BDE-209-induced ERS, autophagy, and apoptosis in MDCC-MSB-1 cells. (A) ROS production in MDCC-MSB-1 cells was detected by the DCFH-DA probe. Scale bar: 200 μm. (B,C) Typical images of immunofluorescence of GRP78 and PERK proteins in MDCC-MSB-1 cells. Scale bar: 50 μm. (D,E) Quantification of the relative fluorescence intensity of GRP78 and PERK proteins. (F) Cluster heat map of mRNA expression changes of ERS-related genes in MDCC-MSB-1 cells after NAC or/and BDE-209 exposure. (G,H) Western blot analysis of ERS-related proteins (ATF6, eIF2α, CHOP, ATF4, and GRP78) in MDCC-MSB-1 cells after NAC or/and BDE-209 exposure. (I,J) Typical images of immunofluorescence of LC3 and Beclin-1 proteins in MDCC-MSB-1 cells. Scale bar: 50 μm. (K,L) Quantification of the relative fluorescence intensity of LC3 and Beclin-1 proteins. (M) Cluster heat map of mRNA expression changes of autophagy-related genes in MDCC-MSB-1 cells after NAC or/and BDE-209 exposure. (N,O) Western blot analysis of autophagy-related proteins in MDCC-MSB-1 cells after NAC or/and BDE-209 exposure. (P) Hoechst 33342 staining. Scale bar: 200 μm. (Q) AO/EB staining. Scale bar: 100 μm. (R) Cluster heat map of mRNA expression changes of apoptosis-related genes in MDCC-MSB-1 cells after NAC or/and BDE-209 exposure. (S,T) Western blot analysis of apoptosis-related proteins in MDCC-MSB-1 cells after NAC or/and BDE-209 exposure. (U) Schematic diagram of grouping of MDCC-MSB-1 cells treated with NAC or/and BDE-209. The data are expressed as means ± SD. Samples indicated a statistically significant difference when represented by distinct superscript letters ($P < 0.05$).

cells in the process of BDE-209 treatment. As shown in Figure 6A, the level of ROS fluorescence in the BDE-209 + NAC group was significantly reduced compared to the BDE-209 group. In addition, the fluorescence intensity of GRP78 (Figure 6B,D) and PERK (Figure 6C,E) proteins in the BDE-209 + NAC group was significantly lower than that in the BDE-209 treatment group alone. The mRNA clustering heat map and Western blot results demonstrate significantly lower mRNA levels of PERK, eIF2α, ATF6, CHOP, GRP78, ATF4, and IRE1 (Figure 6F) and lower protein levels of eIF2α, ATF6, CHOP, GRP78, and ATF4 (Figure 6G,H) in the BDE-209+NAC group compared to the BDE-209 group. Similarly, the fluorescence intensity of the LC3 (Figure 6I,K) and Beclin-1 (Figure 6J,L) proteins in the group treated with BDE-209 + NAC were significantly lower compared to the group treated with BDE-209 alone. Compared to the BDE-209 group, the mRNA levels of LC3, ATG5, and ATG7 in the BDE-209 + NAC group were significantly decreased, and the mRNA expression level of P62 was increased (Figure 6M). At the same time, the change in protein levels detected by Western

https://doi.org/10.1021/acs.jafc.3c09104
J. Agric. Food Chem. 2024, 72, 3741−3754

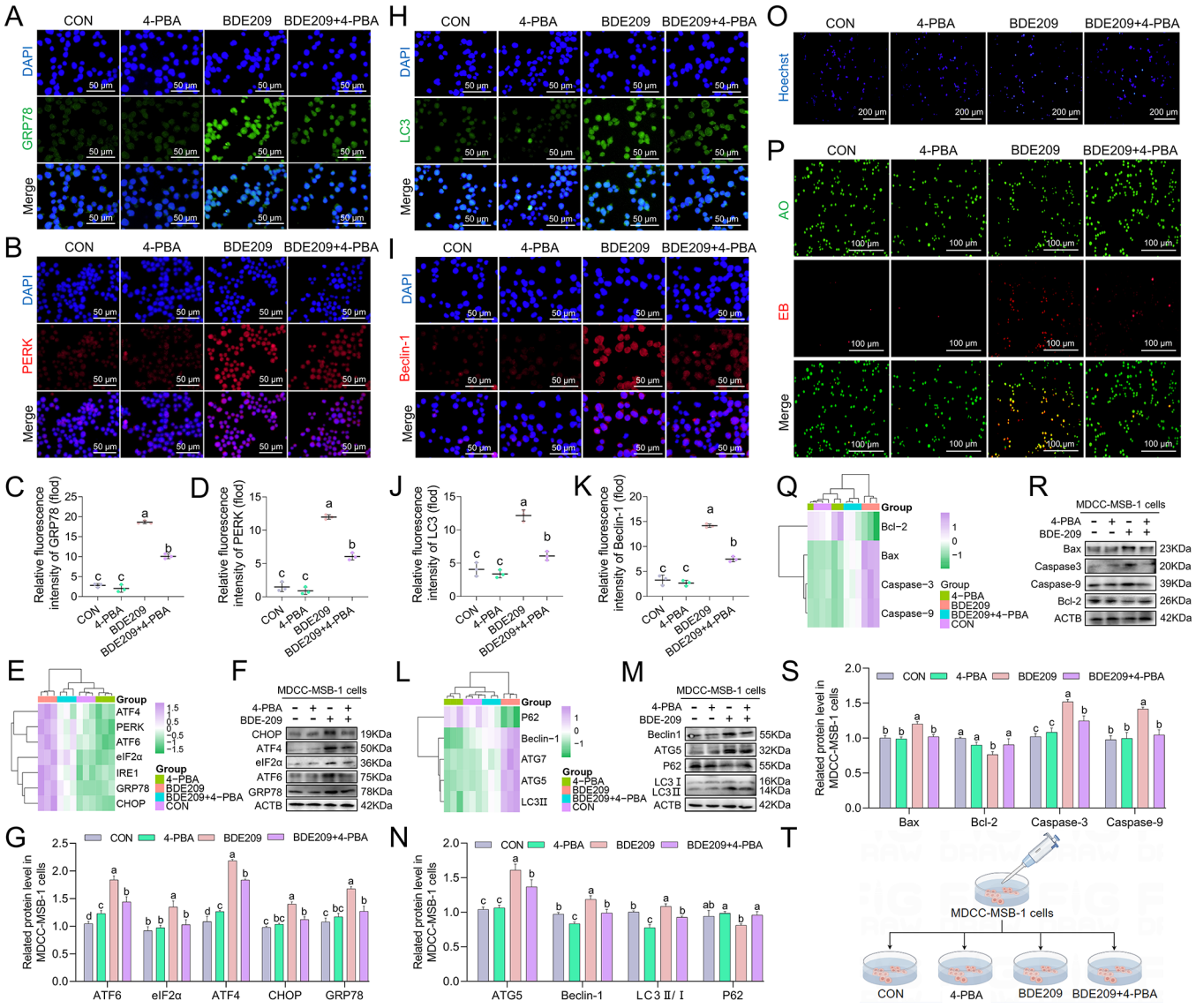

Figure 7. 4-PBA inhibited BDE-209-induced ERS, autophagy, and apoptosis in MDCC-MSB-1 cells. (A,B) Typical images of immunofluorescence of GRP78 and PERK proteins in MDCC-MSB-1 cells. Scale bar: 50 μm. (C,D) Quantification of the relative fluorescence intensity of GRP78 and PERK proteins. (E) Cluster heat map of mRNA expression changes of ERS-related genes in MDCC-MSB-1 cells after 4-PBA or/and BDE-209 exposure. (F,G) Western blot analysis of ERS-related proteins in MDCC-MSB-1 cells after 4-PBA or/and BDE-209 exposure. (H,I) Typical images of immunofluorescence of LC3 and Beclin-1 proteins in MDCC-MSB-1 cells. Scale bar: 50 μm. (J,K) Quantification of the relative fluorescence intensity of LC3 and Beclin-1 proteins. (L) Cluster heat map of mRNA expression changes of autophagy-related genes in MDCC-MSB-1 cells after 4-PBA or/and BDE-209 exposure. (M,N) Western blot analysis of autophagy-related proteins in MDCC-MSB-1 cells after 4-PBA or/and BDE-209 exposure. (O) Hoechst 33342 staining. Scale bar: 200 μm. (P) AO/EB staining. Scale bar: 100 μm. (Q) Cluster heat map of mRNA expression changes of apoptosis-related genes in MDCC-MSB-1 cells after 4-PBA or/and BDE-209 exposure. (R,S) Western blot analysis of apoptosis-related proteins in MDCC-MSB-1 cells after 4-PBA or/and BDE-209 exposure. (T) Schematic diagram of the grouping of MDCC-MSB-1 cells treated with 4-PBA or/and BDE-209. The data are expressed as means ± SD. Samples indicated a statistically significant difference when represented by distinct superscript letters ($P < 0.05$).

blotting was similar to that of mRNA (Figure 6N,O). Compared with the BDE-209 group, NAC treatment decreased the levels of autophagy-related proteins (ATG5, ATG7, and LC3II/I) induced by BDE-209, and increased the levels of P62 protein. In addition, the results of Hoechst 33342 staining (Figure 6P) and AO/EB staining (Figure 6Q) showed that the numbers of apoptosis in the BDE-209 + NAC group were significantly lower than those in the BDE-209 group. Compared with the BDE-209 group, the mRNA (Figure 6R) and protein (Figure 6S,T) levels of proapoptotic markers (Bax, Caspasse-3, and Caspase-9) in the BDE-209 + NAC group were significantly lower, while the mRNA and protein levels of antiapoptotic index Bcl-2 were significantly increased in BDE-209 + NAC group.

3.7. 4-PBA-Alleviated ERS, Autophagy, and Apoptosis Induced by BDE-209 Exposure in MDCC-MSB-1 Cells.

To demonstrate the critical role of ERS in regulating BDE-209-induced autophagy and apoptosis in MDCC-MSB-1 cells, we used 4-PBA, which is a potent ERS inhibitor. Immunofluorescence results showed that the fluorescence intensity of GRP78 (Figure 7A,C) and PERK (Figure 7B,D) proteins in the BDE-209 + 4-PBA group were significantly lower than

https://doi.org/10.1021/acs.jafc.3c09104
J. Agric. Food Chem. 2024, 72, 3741−3754

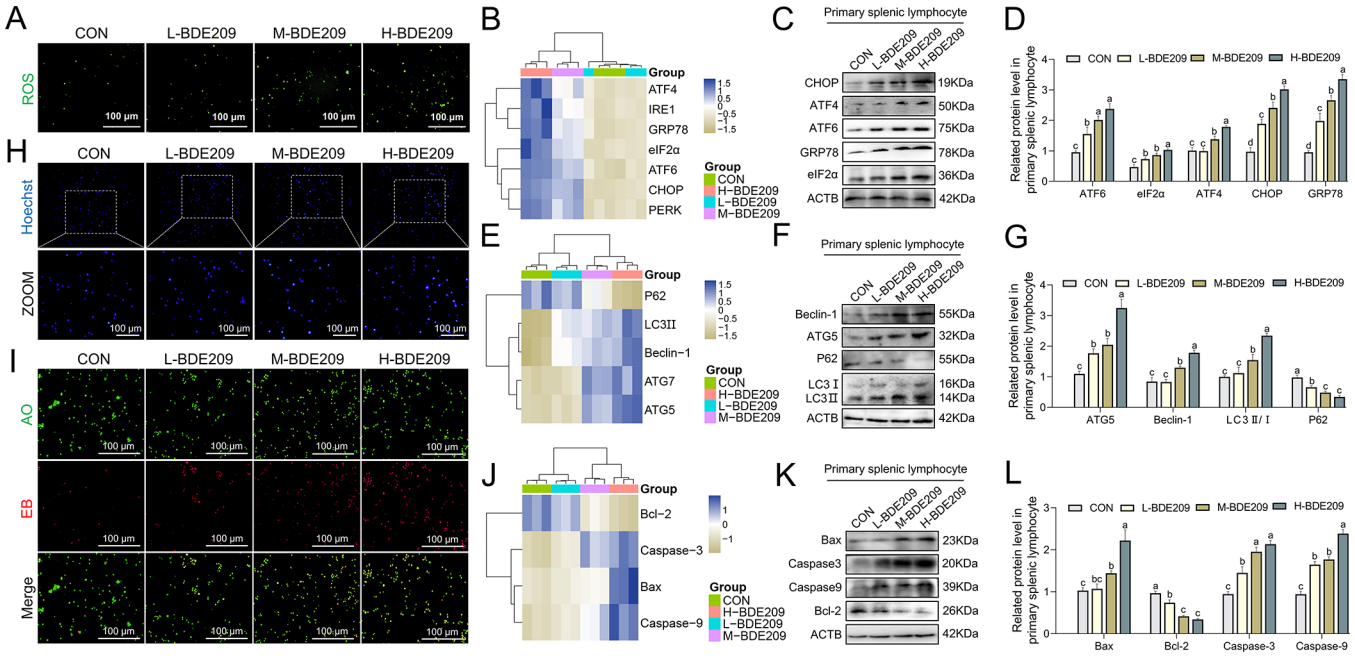

Figure 8. BDE-209 exposure induces oxidative stress, ERS, autophagy, and apoptosis in primary lymphocytes of the chicken spleen. (A) Detection of the ROS level in primary lymphocytes of the chicken spleen after BDE-209 treatment by DCFH-DA staining. Scale bar: 200 μm. (B) Cluster heat map of mRNA expression changes of ERS-related genes in primary lymphocytes of the chicken spleen after BDE-209 exposure. (C,D) Western blot analysis of ERS-related proteins in primary lymphocytes of the chicken spleen after BDE-209 exposure. (E) Cluster heat map of mRNA expression changes of autophagy-related genes in primary lymphocytes of the chicken spleen after BDE-209 exposure. (F,G) Western blot analysis of autophagy stress-related proteins in primary lymphocytes of the chicken spleen after BDE-209 exposure. (H) Hoechst 33342 staining. Scale bar: 100 μm. (I) AO/EB staining. Scale bar: 100 μm. (J) Cluster heat map of mRNA expression changes of apoptosis-related genes in primary lymphocytes of the chicken spleen after BDE-209 exposure. (K,L) Western blot analyses of apoptosis-related proteins in primary lymphocytes of the chicken spleen after BDE-209 exposure. The data are expressed as means ± SD. Samples indicated a statistically significant difference when represented by distinct superscript letters ($P < 0.05$).

those in the BDE-209 group. The heat map of mRNA related to ERS demonstrated that PERK, eIF2α, ATF6, CHOP, GRP78, ATF4, and IRE1 mRNA levels in the BDE-209 + 4-PBA group were significantly lower than those observed in the BDE-209 group (Figure 7E). Subsequently, the detection of ERS-related protein levels showed that BDE-209 could significantly increase the levels of GRP78, eIF2 α, ATF4, ATF6, and CHOP, and most protein levels were recovered after 4-PBA treatment (Figure 7F,G). Similarly, the fluorescence intensities of LC3 (Figure 7H,J) and Beclin-1 (Figure 7I,K) proteins in the BDE-209 + 4-PBA group were significantly lower than those in the BDE-209 treatment group alone. The cluster heat map of autophagy-related mRNA showed that compared with the BDE-209 group, the mRNA levels of LC3, ATG5, and ATG7 in the BDE-209 + 4-PBA group were significantly decreased and the mRNA levels of P62 were increased (Figure 7L). The results of autophagy-associated protein level detection showed that compared with the BDE-209 group, 4-PBA treatment decreased the expression of ATG5, ATG7, and LC3II/I induced by BDE-209, and increased the expression of P62 protein (Figure 7M,N). Next, we evaluated the effect of 4-PBA on BDE-209-induced apoptosis. The results of Hoechst 33342 staining and AO/EB staining showed that the numbers of apoptosis in the BDE-209 + 4-PBA group were significantly lower than those in the BDE-209 group (Figure 7O,P). Compared with the BDE-209 group, the mRNA level of proapoptotic markers (Bax, Caspase-3, and Caspase-9) was significantly decreased, while the mRNA level of antiapoptotic marker Bcl-2 was significantly increased in the BDE-209 + 4-PBA group (Figure 7Q). Interestingly, the expression at the protein level was similar to that at the mRNA level. Compared with the BDE-209 group, the BDE-209 + 4-PBA group could significantly upregulate the expression of Bax, Caspase-3, and Caspase-9 and decrease the levels of Bcl-2 protein at the protein level (Figure 7R,S).

3.8. Effects of BDE-209 Exposure on ERS, Autophagy, and Apoptosis of Primary Chicken Spleen Lymphocytes. The primary lymphocytes of the chicken spleen were used to further verify whether oxidative stress, ERS, autophagy, and apoptosis were the prerequisite factors for BDE-209-induced spleen damage in chickens. First of all, we used a DCFH-DA fluorescent probe to detect the level of intracellular ROS. Compared with the CON group, the BDE-209 exposure group induced an increase in the level of ROS in splenic primary lymphocytes in a dose-dependent manner (Figure 8A). qRT-PCR was used to detect the levels of ERS-related index mRNA in primary lymphocytes of a chicken spleen treated with BDE-209 (Figure 8B). The results showed that the mRNA levels of ATF4, IRE1, GRP78, eIF2α, ATF6, CHOP, and PERK were gradually upregulated with the increase of BDE-209 exposure. In addition, compared to the CON group, the protein levels of CHOP, ATF4, ATF6, GRP78, and eIF2α in spleen primary lymphocytes were significantly increased in a dose-dependent manner (Figure 8C,D). The results of autophagy-related indexes showed that the mRNA expression levels of LC3, Beclin-1, ATG7, and ATG5 in the BDE-209 group were higher than those in the CON group, while the mRNA level of P62 was significantly downregulated (Figure 8E). Similarly, the protein levels of LC3 II/I, Beclin-1, and ATG5 increased, while the protein

https://doi.org/10.1021/acs.jafc.3c09104
J. Agric. Food Chem. 2024, 72, 3741−3754

levels of P62 decreased significantly in the BDE-209-treated group (Figure 8F,G). Hoechst 33342 and AO/EB staining results showed that BDE-209 significantly increased the number of apoptotic cells in a dose-dependent manner (Figure 8H,I). In addition, compared with the CON group, the mRNA levels of Bax, Caspase-3, and Caspase-9 in BDE-209-treated group were significantly upregulated by BDE-209, while the mRNA levels of Bcl-2 was inhibited by BDE-209 (Figure 8J). Western blotting showed similar results at the protein level. BDE-209 exposure decreased the expression of Bcl-2 protein in primary lymphocytes of the chicken spleen while significantly increasing the protein expression of Bax, Caspase-3, and Caspase-9 (Figure 8K,L).

4. DISCUSSION

Exposure to environmental pollutants can easily harm the immune system. After BDE-209 is absorbed into the body, it can not only accumulate in tissues with blood circulation but also form low-bromine compounds through debromination metabolism, thus showing stronger toxic effects.[31,43] In addition, BDE-209 induces cytotoxicity by altering cell membrane parameters and interfering with the cell membrane ligand−receptor network homeostasis. Feng et al. have found that exposure to BDE-209 during pregnancy and lactation can damage the immune function of rats.[44] Exposure to BDE-209 caused pathological damage to the spleen and altered humoral and cellular immunity indices in mice.[45] In this experiment, the BDE-209 exposure model was first utilized to compare with the immunosuppressive positive drug model induced by intramuscular injection of CTX, which demonstrated that BDE-209 exposure could induce spleen damage and suppress immune function in chickens. Second, the regulatory mechanism of BDE-209-induced splenic injury was further investigated by MDCC-MSB-1 cells and the chicken spleen primary lymphocyte BDE-209 exposure model. The results showed that BDE-209 exposure induced increased ROS production, ER swelling, and increased autophagy and apoptosis in chicken lymphocytes. In addition, the use of ROS scavenger (NAC) and ERS inhibitor (4-PBA) significantly reduced the occurrence of ERS, autophagy, and apoptosis in lymphocytes.

The essence of oxidative stress is an imbalance between the generation of ROS and the neutralizing capacity of the antioxidant enzymes. Exposure to environmental pollutants can result in oxidative stress-induced damage in multiple organs throughout the body. Yang et al. demonstrated that exposure to BDE-209 led to a decrease in SOD and CAT activities, as well as an increase in ROS and MDA levels in broiler liver tissue.[46] BDE-209 disrupts the balance between oxidation and antioxidant systems in the mouse colon and ileum by elevating levels of MDA and ROS and reducing antioxidant enzyme activity.[47] Similar to the results of previous studies, we found that BDE-209 exposure increased the MDA content and decreased antioxidant enzyme activity in chicken spleen and MDCC-MSB-1 cells. BDE-209 increased the level of production of ROS in MDCC-MSB-1 cells and splenic primary lymphocytes, and NAC treatment could significantly reduce the level of production of ROS in MDCC-MSB-1. Therefore, our results indicate that BDE-209 exposure can induce oxidative stress in the chicken spleen and increase ROS production in lymphocytes.

The ER plays a significant role in the immune response. The initiation and maintenance of an optimal immune response require efficient protein synthesis, folding, modification, and leukocyte transport, all of which require the ER to participate in coordination. Previous studies have reported that potent zinc activates immunogenic cell death through ROS-mediated ERS.[48] NH3 exposure-induced splenic injury in pigs has also been elucidated about oxidative stress-mediated ERS.[49] In this study, TEM showed that BDE-209 exposure could cause swelling of the ER in the chicken spleen. In addition, BDE-209 exposure significantly upregulated the expression levels of ERS-related markers in the spleen and lymphocytes. This may be due to the fact that BDE-209 exposure triggers ROS overaccumulation increasing the number of misfolded proteins in the ER, which in turn leads to the occurrence of ERS and impairment of organelle function.[50] Similarly, both the brominated flame retardants BDE-47 and DBDPE were able to upregulate the expression of ERS-related marker genes in cells by inducing ROS accumulation.[51,52] Thus, it is speculated that ERS could be a shared biological impact of diverse brominated flame retardants. Interestingly, NAC or 4-PBA treatment significantly reduced the upward trend of ERS-related genes. This further confirms that BDE-209 exposure triggers ERS in the spleen via the ROS pathway.

There is a complex link between ERS and autophagy. Autophagy will be activated when the amount of misfolded or unfolded proteins in the cell exceeds the ability of enzymes to degrade them. In this study, TEM observations revealed that exposure to BDE-209 increased the proportion of autophagosomes. In addition, BDE-209 treatment altered the expression levels of intracellular autophagy-related factors LC3, P62, ATG5, ATG7, and Beclin-1 genes. These results suggest that exposure to BDE-209 activates autophagy in the spleen and lymphocytes. In addition to detecting changes in autophagy-related metrics, we also evaluated the relationship between ERS and autophagy in the presence of BDE-209. It has been shown that PERK and its downstream factors ATF4 and CHOP can stimulate autophagy and degrade proteins to counter ERS-induced cytotoxicity.[53] In contrast, IRE1 was shown to inhibit the activation of autophagy in the ERS state.[24] In the study presented here, BDE-209 exposure significantly increased the gene expression levels of PERK, ATF4, CHOP, and IRE1. NAC and 4-PBA pretreatment not only significantly inhibited ERS levels but also significantly inhibited the increase in autophagy. This suggests that ERS may be the upstream mechanism of BDE-209-induced autophagy rather than inhibition, which may be due to the dominant role of the PERK pathway in autophagy regulation.[23] Li et al. demonstrated that GRP78 and Beclin-1 proteins play important roles in ERS-induced autophagy.[54] Activated ATF6 protein regulates the expression of downstream autophagy-related genes during ERS, leading to the activation of the autophagy pathway, which triggers hepatic steatosis.[55] In our study, BDE-209 exposure significantly increased the expression levels of GRP78, Beclin-1, and ATF6, which may also be an important factor in the increase in autophagy induced by BDE-209 exposure. Furthermore, previous studies reported that BDE-209 exposure induced autophagy in HUVEC cells via the ERS pathway, which is consistent with our results.[12] Thus, our results suggest that BDE-209 treatment can activate cellular autophagy via the ROS-mediated ERS pathway.

ERS has been shown to be involved in the regulation of programmed cell death and plays an important role in the development of various diseases or injuries. As an adaptive mechanism, mild ERS helps to restore ER homeostasis to

https://doi.org/10.1021/acs.jafc.3c09104
J. Agric. Food Chem. 2024, 72, 3741−3754

promote cell survival. However, excessive ERS can lead to apoptosis.[54] In this study, TEM results showed nuclear membrane crumpling, increased electron density, incomplete mitochondrial cristae, and the presence of apoptotic vesicles in the BDE-209 group. BDE-209 exposure significantly upregulated the expression levels of apoptosis-related genes. The above results were also validated in the previously reported results of PBDE-induced apoptosis and injury of immune cells.[56] In addition to detecting changes in apoptosis-related indicators, we also evaluated the relationship between ERS and apoptosis. Interestingly, treatment with either NAC or 4-PBA significantly alleviated apoptosis. The possible reason for this is that Bax and Bcl-2 can be involved in sensing ER homeostasis, and ERS occurs when the expression of Bax and Bcl-2 is interfered with and apoptosis is induced. The other reason is that after BDE-209 exposure, PERK, IRE1, and ATF6 receptor factors are activated in lymphocytes, which segregate from GRP78. IRE1α can induce apoptosis by promoting the activation of the relevant signaling pathways, and PERK can increase the translation of ATF4 or ATF6 by phosphorylating eIF2α, which can activate the transcription of CHOP genes to promote cellular apoptosis.[57] In conclusion, the results of this study suggest that BDE-209 exposure can induce apoptosis through the ROS-mediated ERS pathway.

Autophagy, as a cellular self-protection mechanism, plays an important role in regulating cell survival and death. The crosstalk between autophagy and apoptosis has also been elucidated in several studies. During myogenic differentiation, increased apoptosis activates autophagy, which is enhanced to prevent excessive apoptosis and maintain cell stability.[58] Cr(VI) exposure can induce crosstalk between apoptosis and autophagy in A549 cells by triggering ERS.[59] Undeniably, given the complexity of the molecular interactions, further experiments are needed to determine the specific modes of regulation between autophagy and apoptosis under BDE-209 exposure. In conclusion, the present results of this study indicate that BDE-209 treatment can activate autophagy and apoptosis in the chicken spleen and lymphocytes via the ROS-mediated ERS pathway. These results not only partially revealed the toxicological mechanism of BDE-209-induced splenic injury in avian species but also provided new references for further studies on the toxicity mechanism of BDE-209 on avian immune organs as well as the protection of ecological environment and animal health.

■ ASSOCIATED CONTENT

Supporting Information

The Supporting Information is available free of charge at https://pubs.acs.org/doi/10.1021/acs.jafc.3c09104.

Sequence of primers for qRT-PCR; information of antibodies used in Western blot and immunofluorescence; and clustering heat map of mRNA expression levels of antimicrobial peptides and immunoglobulins in chicken spleen after BDE-209 exposure (PDF)

■ AUTHOR INFORMATION

Corresponding Author

Ziwei Zhang − *College of Veterinary Medicine and Key Laboratory of the Provincial Education, Department of Heilongjiang for Common Animal Disease Prevention and Treatment, College of Veterinary Medicine, Northeast Agricultural University, Harbin 150030, PR China;* orcid.org/0000-0002-5705-4611; Email: zhangziwei@neau.edu.cn

Authors

Bendong Shi − *College of Veterinary Medicine, Northeast Agricultural University, Harbin 150030, PR China*

Bowen Dong − *College of Veterinary Medicine, Northeast Agricultural University, Harbin 150030, PR China*

Jianhua Shan − *College of Veterinary Medicine, Northeast Agricultural University, Harbin 150030, PR China*

Zhuoqi Zhang − *College of Veterinary Medicine, Northeast Agricultural University, Harbin 150030, PR China*

Qiaohan Liu − *College of Veterinary Medicine, Northeast Agricultural University, Harbin 150030, PR China*

Yangyang Jiang − *College of Veterinary Medicine, Northeast Agricultural University, Harbin 150030, PR China*

Cheng Fang − *College of Veterinary Medicine, Northeast Agricultural University, Harbin 150030, PR China*

Jingzeng Cai − *College of Veterinary Medicine, Northeast Agricultural University, Harbin 150030, PR China*

Complete contact information is available at: https://pubs.acs.org/10.1021/acs.jafc.3c09104

Author Contributions

B.S.: design experiment, writing-original draft. J.S. and Z.Z.: data curation, methodology. Q.L. and C.F.: investigation, software. B.D. and Y.J.: methodology, supervision. J.C.: conceptualization, supervision. Z.Z.: funding acquisition, writing-review, and editing.

Notes

The authors declare no competing financial interest.

■ ACKNOWLEDGMENTS

This study was supported by the Excellent Youth Foundation of Heilongjiang Province of China. (YQ2021C021); "2023 Young Leading Talents" Project of Northeast Agricultural University (NEAU2023QNLJ-012).

■ REFERENCES

(1) Wang, J.; Yan, Z.; Zheng, X.; Wang, S.; Fan, J.; Sun, Q.; Xu, J.; Men, S. Health risk assessment and development of human health ambient water quality criteria for PBDEs in China. *Sci. Total Environ.* **2021**, *799*, No. 149353.

(2) Ni, K.; Lu, Y.; Wang, T.; Kannan, K.; Gosens, J.; Xu, L.; Li, Q.; Wang, L.; Liu, S. A review of human exposure to polybrominated diphenyl ethers (PBDEs) in China. *Int. J. Hyg Environ. Health* **2013**, *216* (6), 607−623.

(3) Zheng, X. B.; Luo, X. J.; Zheng, J.; Zeng, Y. H.; Mai, B. X. Contaminant sources, gastrointestinal absorption, and tissue distribution of organohalogenated pollutants in chicken from an e-waste site. *Sci. Total Environ.* **2015**, *505*, 1003−1010.

(4) Wang, D. H.; Ma, H. M.; Chen, Z. L.; Shi, G. T. Occurrences and possible sources of persistent organic pollutants (POPs) in ice-free area soils in East Antarctica. *Catena* **2022**, *212*, No. 106083.

(5) Yeo, B. G.; Takada, H.; Yamashita, R.; Okazaki, Y.; Uchida, K.; Tokai, T.; Tanaka, K.; Trenholm, N. PCBs and PBDEs in microplastic particles and zooplankton in open water in the Pacific Ocean and around the coast of Japan. *Mar. Pollut. Bull.* **2020**, *151*, No. 110806.

(6) Lee, H. K.; Lee, S.; Lim, J. E.; Moon, H. B. Legacy and novel flame retardants in water and sediment from highly industrialized bays of Korea: Occurrence, source tracking, decadal time trend, and ecological risks. *Mar. Pollut. Bull.* **2020**, *160*, No. 111639.

(7) Ji, X.; Ding, J.; Xie, X.; Cheng, Y.; Huang, Y.; Qin, L.; Han, C. Pollution Status and Human Exposure of Decabromodiphenyl Ether (BDE-209) in China. *ACS Omega* **2017**, *2* (7), 3333−3348.

(8) Wang, Y.; Wang, X.; Sui, S.; Liu, Z. Endocrine disrupting and carcinogenic effects of decabromodiphenyl ether. *Front. Endocrinol.* **2023**, *14*, No. 1183815.
(9) Yang, Y.; Zhu, X.; Rao, Q.; Liu, Z.; Yang, J.; Zhao, Z. Toxicokinetics and edible tissues-specific bioaccumulation of decabrominated diphenyl ethers (BDE-209) after exposure to the broilers. *Ecotoxicol Environ. Saf* **2022**, *248*, No. 114324.
(10) Li, X.; Zhang, Y.; Gao, L.; Yang, X.; Zhou, G.; Sang, Y.; Xue, J.; Shi, Z.; Sun, Z.; Zhou, X. BDE-209 induced spermatogenesis disorder by inhibiting SETD8/H4K20me1 related histone methylation in mice. *Sci. Total Environ.* **2023**, *864*, No. 161162.
(11) Zhao, Y.; Fan, K.; Zhu, Y.; Zhao, Y.; Cai, J.; Jin, L. Gestational exposure to BDE-209 induces placental injury via the endoplasmic reticulum stress-mediated PERK/ATF4/CHOP signaling pathway. *Ecotoxicol Environ. Saf* **2022**, *233*, No. 113307.
(12) Hou, Y.; Fu, J.; Sun, S.; Jin, Y.; Wang, X.; Zhang, L. BDE-209 induces autophagy and apoptosis via IRE1alpha/Akt/mTOR signaling pathway in human umbilical vein endothelial cells. *Environ. Pollut.* **2019**, *253*, 429−438.
(13) Che, S.; Chen, S.; Li, S.; Ruan, Z. Decabromodiphenyl ether initiates mitochondria-dependent apoptosis by disrupting calcium homeostasis in mice livers. *Chemosphere* **2022**, *291* (Pt 1), No. 132767.
(14) Li, J.; Yin, K.; Hou, L.; Zhang, Y.; Lu, H.; Ma, C.; Xing, M. Polystyrene microplastics mediate inflammatory responses in the chicken thymus by Nrf2/NF-kappaB pathway and trigger autophagy and apoptosis. *Environ. Toxicol Pharmacol* **2023**, *100*, No. 104136.
(15) Shah, S. W. A.; Chen, J.; Han, Q.; Xu, Y.; Ishfaq, M.; Teng, X. Ammonia inhalation impaired immune function and mitochondrial integrity in the broilers bursa of fabricius: Implication of oxidative stress and apoptosis. *Ecotoxicol Environ. Saf* **2020**, *190*, No. 110078.
(16) Li, H. Y.; Huang, L. F.; Huang, X. R.; Wu, D.; Chen, X. C.; Tang, J. X.; An, N.; Liu, H. F.; Yang, C. Endoplasmic Reticulum Stress in Systemic Lupus Erythematosus and Lupus Nephritis: Potential Therapeutic Target. *J. Immunol Res.* **2023**, *2023*, No. 7625817.
(17) Zhang, K.; Liao, J.; Hu, Z.; Li, Q.; Hu, L.; Guo, J.; Li, Y.; Zhang, H.; Pan, J.; Tang, Z. Mitochondria-mediated apoptosis and endoplasmic reticulum stress are involved in the toxicity induced by copper in the porcine spleen. *Environ. Sci. Pollut Res. Int.* **2023**, *30* (41), 94928−94939.
(18) Guo, H.; Hu, R.; Huang, G.; Pu, W.; Chu, X.; Xing, C.; Zhang, C. Molybdenum and cadmium co-exposure induces endoplasmic reticulum stress-mediated apoptosis by Th1 polarization in Shaoxing duck (Anas platyrhyncha) spleens. *Chemosphere* **2022**, *298*, No. 134275.
(19) Li, P.; Gao, H.; Dong, L.; Liu, L.; Zhou, G.; Luo, C.; Tian, Z.; Xia, T.; Wang, A.; Zhang, S. Perinatal low-dose PBDE-47 exposure hampered thyroglobulin turnover and induced thyroid cell apoptosis by triggering ER stress and lysosomal destabilization contributing to thyroid toxicity in adult female rats. *J. Hazard Mater.* **2020**, *392*, No. 122265.
(20) Kwon, J.; Kim, J.; Kim, K. I. Crosstalk between endoplasmic reticulum stress response and autophagy in human diseases. *Anim Cells Syst. (Seoul)* **2023**, *27* (1), 29−37.
(21) Prerna, K.; Dubey, V. K. Beclin1-mediated interplay between autophagy and apoptosis: New understanding. *Int. J. Biol. Macromol.* **2022**, *204*, 258−273.
(22) Di, Y. Q.; Han, X. L.; Kang, X. L.; Wang, D.; Chen, C. H.; Wang, J. X.; Zhao, X. F. Autophagy triggers CTSD (cathepsin D) maturation and localization inside cells to promote apoptosis. *Autophagy* **2021**, *17* (5), 1170−1192.
(23) Zhao, L.; Wang, L.; Wang, H.; Xi, T.; Liu, S.; Li, Y.; Ruan, J.; Huang, Y. Endoplasmic reticulum chaperone GRP78 participates in fluoride-induced autophagy in LS8 cells by regulating the IRE1-TRAF2-JNK pathway. *Environ. Toxicol* **2023**, *38* (7), 1756−1767.
(24) Li, Z.; Huang, Z.; Zhang, H.; Lu, J.; Wei, Y.; Yang, Y.; Bai, L. IRE1-mTOR-PERK Axis Coordinates Autophagy and ER Stress-Apoptosis Induced by P2 × 7-Mediated Ca(2+) Influx in Osteoarthritis. *Front Cell Dev Biol.* **2021**, *9*, No. 695041.
(25) Pu, L.; Yi, F.; Yu, W. J.; Li, Y. J.; Tu, Y. H.; Xu, A. H.; Wang, Y. Endoplasmic reticulum stress mediates environmental particle-induced inflammatory response in bronchial epithelium. *J. Immunotoxicol.* **2023**, *20* (1), No. 2229428.
(26) Liu, R. P.; He, S. Y.; Wang, J.; Wang, X. Q.; Jin, Z. L.; Guo, H.; Wang, C. R.; Xu, Y. N.; Kim, N. H. BDE-47 Induces Mitochondrial Dysfunction and Endoplasmic Reticulum Stress to Inhibit Early Porcine Embryonic Development. *Animals* **2023**, *13* (14), 2291.
(27) Rockel, J. S.; Kapoor, M. Autophagy: controlling cell fate in rheumatic diseases. *Nat. Rev. Rheumatol* **2016**, *12* (9), 517−531.
(28) Bettigole, S. E.; Glimcher, L. H. Endoplasmic reticulum stress in immunity. *Annu. Rev. Immunol.* **2015**, *33*, 107−138.
(29) Wang, J.; Tang, J.; Li, X.; Ning, X.; Sun, C.; Zhang, N.; Zhang, S. Curcumin alleviates spleen immunotoxicity induced by decabrominated diphenyl ethers (BDE-209) by improving immune function and inhibiting inflammation and apoptosis in broilers. *Ecotoxicol Environ. Saf* **2023**, *259*, No. 115048.
(30) Khani, L.; Martin, L.; Pulaski, L. Cellular and physiological mechanisms of halogenated and organophosphorus flame retardant toxicity. *Sci. Total Environ.* **2023**, *897*, No. 165272.
(31) Cheng, L.; Rao, Q.; Zhang, Q.; Song, W.; Guan, S.; Jiang, Z.; Wu, T.; Zhao, Z.; Song, W. The immunotoxicity of decabromodiphenyl ether (BDE-209) on broiler chicks by transcriptome profiling analysis. *Ecotoxicol Environ. Saf* **2022**, *232*, No. 113284.
(32) Sun, S.; Jin, Y.; Yang, J.; Zhao, Z.; Rao, Q. Nephrotoxicity and possible mechanisms of decabrominated diphenyl ethers (BDE-209) exposure to kidney in broilers. *Ecotoxicol Environ. Saf* **2021**, *208*, No. 111638.
(33) Guo, L.; Liu, J.; Hu, Y.; Wang, D.; Li, Z.; Zhang, J.; Qin, T.; Liu, X.; Liu, C.; Zhao, X.; Fan, Y. P.; Han, G.; Nguyen, T. L. Astragalus polysaccharide and sulfated epimedium polysaccharide synergistically resist the immunosuppression. *Carbohydr. Polym.* **2012**, *90* (2), 1055−1060.
(34) Yin, K.; Wang, D.; Zhao, H.; Wang, Y.; Zhang, Y.; Liu, Y.; Li, B.; Xing, M. Polystyrene microplastics up-regulates liver glutamine and glutamate synthesis and promotes autophagy-dependent ferroptosis and apoptosis in the cerebellum through the liver-brain axis. *Environ. Pollut.* **2022**, *307*, No. 119449.
(35) Roman, L.; Lowenstine, L.; Parsley, L. M.; Wilcox, C.; Hardesty, B. D.; Gilardi, K.; Hindell, M. Is plastic ingestion in birds as toxic as we think? Insights from a plastic feeding experiment. *Sci. Total Environ.* **2019**, *665*, 660−667.
(36) Dong, B.; Jiang, Y.; Shi, B.; Zhang, Z.; Zhang, Z. Selenomethionine alleviates decabromodiphenyl ether-induced oxidative stress and ferroptosis via the NRF2/GPX4 pathway in the chicken brain. *J. Hazard Mater.* **2024**, *465*, No. 133307.
(37) Jiang, Y.; Dong, B.; Jiao, X.; Shan, J.; Fang, C.; Zhang, K.; Li, D.; Xu, C.; Zhang, Z. Nano-selenium alleviates the pyroptosis of cardiovascular endothelial cells in chicken induced by decabromodiphenyl ether through ERS-TXNIP-NLRP3 pathway. *Sci. Total Environ.* **2024**, *915*, No. 170129.
(38) Ren, Z.; Wang, Y.; Deng, H.; Deng, Y.; Deng, J.; Zuo, Z.; Wang, Y.; Peng, X.; Cui, H.; Shen, L.; Ma, X.; Fang, J. Deoxynivalenol-induced cytokines and related genes in concanavalin A-stimulated primary chicken splenic lymphocytes. *Toxicol In Vitro* **2015**, *29* (3), 558−563.
(39) Cai, J.; Liu, P.; Zhang, X.; Shi, B.; Jiang, Y.; Qiao, S.; Liu, Q.; Fang, C.; Zhang, Z. Micro-algal astaxanthin improves lambda-cyhalothrin-induced necroptosis and inflammatory responses via the ROS-mediated NF-kappaB signaling in lymphocytes of carp (Cyprinus carpio L.). *Fish Shellfish Immunol* **2023**, *139*, No. 108929.
(40) Li, D.; Zhang, K.; Xu, C.; Jiang, Y.; Shan, J.; Zhang, Z.; Cai, J. Cypermethrin induces apoptosis, autophagy and inflammation via ERS-ROS-NF-kappaB axis in hepatocytes of carp (Cyprinus carpio). *Pestic. Biochem. Physiol.* **2023**, *196*, No. 105625.
(41) Cai, J.; Guan, H.; Li, D.; Shi, B.; Jiang, Y.; Qiao, S.; Liu, Q.; Fang, C.; Zhang, Z. New insights into Microalgal astaxanthin's effect on Lambda-cyhalothrin-induced lymphocytes immunotoxicity in Cyprinus carpio: Involving miRNA-194−5p-FoxO1-mediated-mi-

https://doi.org/10.1021/acs.jafc.3c09104
J. Agric. Food Chem. 2024, 72, 3741−3754

tophagy and pyroptosis. *Fish Shellfish Immunol* **2023**, *141*, No. 109046.
(42) Lian, C. Y.; Chu, B. X.; Xia, W. H.; Wang, Z. Y.; Fan, R. F.; Wang, L. Persistent activation of Nrf2 in a p62-dependent non-canonical manner aggravates lead-induced kidney injury by promoting apoptosis and inhibiting autophagy. *J. Adv. Res.* **2023**, *46*, 87−100.
(43) Motamedi, M.; Yerushalmi, L.; Haghighat, F.; Chen, Z. A critical review of water contamination by polybrominated diphenyl ethers (PBDE) and main degradation techniques. *J. Environ. Chem. Eng.* **2022**, *10* (4), No. 108196.
(44) Liu, X.; Zhan, H.; Zeng, X.; Zhang, C.; Chen, D. The PBDE-209 exposure during pregnancy and lactation impairs immune function in rats. *Mediators Inflamm.* **2012**, *2012*, No. 692467.
(45) Liao, T.; Li, B.; Zhang, Z.; Feng, W.; Chen, Y.; Ding, Y.; Chen, H.; Zhao, T.; Mao, G.; Wu, X.; Yang, L. Short-term exposure of decabromodiphenyl ether in female adult Balb/c mice: Immune toxicity and self-recovery. *Toxicol. Lett.* **2021**, *342*, 26−37.
(46) Yang, Y.; Jin, Y.; Zhu, X.; Rao, Q.; Zhao, Z.; Yang, J. Hepatotoxicity evaluation and possible mechanisms of decabrominated diphenyl ethers (BDE-209) in broilers: Oxidative stress, inflammatory, and transcriptomics. *Ecotoxicol Environ. Saf* **2023**, *264*, No. 115460.
(47) Shaoyong, W. K.; Zhang, W. R.; Wang, C. Y.; Kou, Z. Y.; Yong, W. L.; Jiao, J. H.; Yan, W. Y.; Pang, W. J. BDE-209 caused gut toxicity through modulating the intestinal barrier, oxidative stress, autophagy, inflammation, and apoptosis in mice. *Sci. Total Environ.* **2021**, *776*, No. 146018.
(48) Liao, L. S.; Chen, Y.; Hou, C.; Liu, Y. H.; Su, G. F.; Liang, H.; Chen, Z. F. Potent Zinc(II)-Based Immunogenic Cell Death Inducer Triggered by ROS-Mediated ERS and Mitochondrial Ca(2+) Overload. *J. Med. Chem.* **2023**, *66* (15), 10497−10509.
(49) Zhou, S.; Zhang, X.; Fu, Q.; Cheng, Z.; Ji, W.; Liu, H. The use of selenomethionine to reduce ammonia toxicity in porcine spleen by inhibiting endoplasmic reticulum stress and autophagy mediated by oxidative stress. *Ecotoxicol Environ. Saf* **2022**, *242*, No. 113887.
(50) Ong, G.; Logue, S. E. Unfolding the Interactions between Endoplasmic Reticulum Stress and Oxidative Stress. *Antioxidants* **2023**, *12* (5), 981.
(51) Jiang, C.; Zhang, S.; Liu, H.; Zeng, Q.; Xia, T.; Chen, Y.; Kuang, G.; Zhao, G.; Wu, X.; Zhang, X.; Wang, A. The role of the IRE1 pathway in PBDE-47-induced toxicity in human neuroblastoma SH-SY5Y cells in vitro. *Toxicol. Lett.* **2012**, *211* (3), 325−333.
(52) Jing, L.; Sun, Y.; Wang, J.; Zhou, X.; Shi, Z. Oxidative stress and endoplasmic reticulum stress contributed to hepatotoxicity of decabromodiphenyl ethane (DBDPE) in L-02 cells. *Chemosphere* **2022**, *286* (Pt 1), No. 131550.
(53) Zielke, S.; Kardo, S.; Zein, L.; Mari, M.; Covarrubias-Pinto, A.; Kinzler, M. N.; Meyer, N.; Stolz, A.; Fulda, S.; Reggiori, F.; Kogel, D.; van Wijk, S. ATF4 links ER stress with reticulophagy in glioblastoma cells. *Autophagy* **2021**, *17* (9), 2432−2448.
(54) Hetz, C. The unfolded protein response: controlling cell fate decisions under ER stress and beyond. *Nat. Rev. Mol. Cell Biol.* **2012**, *13* (2), 89−102.
(55) Munoz-Guardiola, P.; Casas, J.; Megias-Roda, E.; Sole, S.; Perez-Montoyo, H.; Yeste-Velasco, M.; Erazo, T.; Dieguez-Martinez, N.; Espinosa-Gil, S.; Munoz-Pinedo, C.; Yoldi, G.; Abad, J. L.; Segura, M. F.; Moran, T.; Romeo, M.; Bosch-Barrera, J.; Oaknin, A.; Alfon, J.; Domenech, C.; Fabrias, G.; Velasco, G.; Lizcano, J. M. The anti-cancer drug ABTL0812 induces ER stress-mediated cytotoxic autophagy by increasing dihydroceramide levels in cancer cells. *Autophagy* **2021**, *17* (6), 1349−1366.
(56) Lv, Q. Y.; Wan, B.; Guo, L. H.; Zhao, L.; Yang, Y. In vitro immune toxicity of polybrominated diphenyl ethers on murine peritoneal macrophages: apoptosis and immune cell dysfunction. *Chemosphere* **2015**, *120*, 621−630.
(57) Wang, Z.; Liu, S.; Cheng, Z.; Xu, G.; Li, F.; Bu, Q.; Zhang, L.; Song, Y.; An, X. Endoplasmic reticulum stress exacerbates microplastics-induced toxicity in animal cells. *Food Res. Int.* **2024**, *175*, No. 113818.
(58) Jiang, A. W.; Guo, H. Y.; Wu, W. J.; Liu, H. L. The Crosstalk between Autophagy and Apoptosis Is Necessary for Myogenic Differentiation. *J. Agr Food Chem.* **2021**, *69* (13), 3942−3951.
(59) Ge, H.; Li, Z.; Jiang, L.; Li, Q.; Geng, C.; Yao, X.; Shi, X.; Liu, Y.; Cao, J. Cr (VI) induces crosstalk between apoptosis and autophagy through endoplasmic reticulum stress in A549 cells. *Chem. Biol. Interact* **2019**, *298*, 35−42.

https://doi.org/10.1021/acs.jafc.3c09104
J. Agric. Food Chem. 2024, 72, 3741−3754